Concentration-dependent surface-enhanced resonance Raman scattering of a porphyrin derivative adsorbed on colloidal silver particles

ARTICLE *in* JOURNAL OF COLLOID AND INTERFACE SCIENCE · AUGUST 2003

Impact Factor: 3.37 · DOI: 10.1016/S0021-9797(03)00022-5 · Source: PubMed

4 AUTHORS, INCLUDING:

Joydeep Chowdhury
Jadavpur University
71 PUBLICATIONS **631** CITATIONS

SEE PROFILE

Manash Ghosh
Indian Association for the Cultivation of Sci…
57 PUBLICATIONS **621** CITATIONS

SEE PROFILE

Prabir Pal
Indian Association for the Cultivation of Sci…
73 PUBLICATIONS **806** CITATIONS

SEE PROFILE

ACADEMIC PRESS

Available online at www.sciencedirect.com
SCIENCE DIRECT®

Journal of Colloid and Interface Science 263 (2003) 318–326

JOURNAL OF Colloid and Interface Science

www.elsevier.com/locate/jcis

Concentration-dependent surface-enhanced resonance Raman scattering of a porphyrin derivative adsorbed on colloidal silver particles

Joydeep Chowdhury,[a] Manash Ghosh,[b] Prabir Pal,[b,*] and T.N. Misra [b]

[a] *Department of Physics, Sammilani Mahavidyalaya, Baghajatin Station, E.M. Bypass, Kolkata 700 075, India*
[b] *Department of Spectroscopy, Indian Association for the Cultivation of Science, Kolkata 700 032, India*

Received 3 October 2002; accepted 3 January 2003

Abstract

Surface-enhanced Raman spectra (SERS) of 5,10,15,20-tetrakis(1-decylpyridium-4-yl)-21H,23H-porphintetrabromide or Por 10 (H_2Tdpyp) adsorbed on silver hydrosols are compared with the FTIR and resonance Raman spectrum (RRS) in the bulk and in solution. Comparative analysis of the RR and the FTIR spectra indicate that the molecule, in its free state, has D_{2h} symmetry rather than C_{2v}. The SERS spectra, obtained on adsorption of this molecule on borohydride-reduced silver sol, indicate the formation of silver porphyrin. With the change in the adsorbate concentration, the SERS shows that the molecule changes its orientation on the colloidal silver surface. The appearance of longer wavelength band in the electronic absorption spectra of the sol has been attributed to the coagulation of colloidal silver particles in the sol. The long wavelength band is found to be red-shifted with the decrease in adsorbate concentration. The excitation profile study indicates that the resonance of the Raman excitation radiation with the original sol band is more important than that with the new aggregation band for the SERS activity. This indicates a large contribution of electromagnetic effect to surface enhancement.

Keywords: Surface-enhanced Raman scattering; Silver colloid; Charge transfer; Light scattering

1. Introduction

Photosynthetic proteins contain ordered assemblies of porphyrinic molecules (chlorophylls), which serve as the active species at the initial steps of light-energy conversion [1,2]. The electronic structure of these assemblies facilitates extremely fast, vectorial electron transfer during the primary charge separation [3]. Moreover, exogenous porphyrin molecules are of interest in biochemistry owing to their potential applications in photodynamic therapy (PDT) of cancer. The first PDT drug to be approved by the FDA for clinical use in the United States is photofrin, a complex mixture of different forms of hematoporphyrin. It also find applications in various antiviral treatment and in molecular biopsy involved in the selective cleavage of nucleic acids and in the specific sensing of DNA sequences [4,5]. Consequently, the elucidation of the structural organization and photophysics of the porphyrin molecules at extremely low concentration, close to those encountered under physiological conditions and in ordered molecular assemblies [6], is a topic of current interest.

Over the past decade there have been extensive reports on the Raman scattering (RS) and the resonance Raman scattering (RRS) of free base and metal porphyrins [7–20], which mainly focus on the nature of the chemical bonds and the geometrical details of the molecules. Since resonance Raman (RR) technique offers a means of selectively enhancing certain vibrational modes which provide unique and important information about the nature of the chemical bonds, electronic states, core size, ligation states, environmental effects, etc., RRS spectra of porphyrins and metalloporphyrins have been extensively investigated and have resulted in useful correlations between Raman frequencies and various stereochemical parameters.

Here, we report the concentration-dependent surface-enhanced resonance Raman scattering (SERRS) of 5,10,15,20-tetrakis(1-decylpyridium-4-yl)-21H,23H-porphintetrabromide (H_2Tdpyp) or Por 10 adsorbed on colloidal silver particles. Surface-enhanced Raman scattering (SERS) is a useful technique for studying the nature of physical and chemical adsorption of molecules on the metals. With

* Corresponding author.
E-mail address: prabirkumarpal@hotmail.com (P. Pal).

0021-9797/03/$ – see front matter
doi:10.1016/S0021-9797(03)00022-5

the vibrational information available from this technique, the molecular forms and the orientation of adsorbed species on the metal surfaces can be investigated. The theoretical treatment of SERS principally falls into two distinct classes [21–23]. Chemical effects invoke direct contact and charge transfer between the adsorbate and the metal surface and predict primarily short-range enhancement. Electromagnetic (EM) effect, on the other hand, predicts long-range enhancement effects and is based on the plasmon resonance of the metal surface. Earlier reports on the SER spectra of porphyrin derivatives mainly focused on the metallation and orientation of the molecule on the silver surface [4–30]. Laser-ablated Ag colloids, modified by mercapto acetate spacers, have been reported as substrates for the SERRS spectra of cationic free-base porphyrin species [31]. Recently, suppression of antisymmetric scattering, antiresonance, and higher order scattering effect on water-insoluble Ni(II) porphin adsorbed on aqueous silver sol has been reported [32].

The reports on the molecular concentration dependence of SER spectra are limited [33–39]. In these studies the changes in the SER spectral profile with the concentration of the molecules adsorbed on the silver colloidal surface has been attributed to the change in the molecular orientation.

2. Experimental

2.1. Chemicals and procedure

H_2Tdpyp was synthesized and purified according to Okino et al. [40]. Purity of the synthesized H_2Tdpyp was estimated to be ≈99% as verified by thin-layer chromatography. The molecule is soluble in water at 1.0×10^{-4} M or lower concentration. Stable silver sol was prepared according to the process of Creighton et al. [41]. The stable yellowish sol thus prepared shows a single extinction maximum at 392 nm. The size of the silver particles in such sol is known to be in the 1- to 50-nm range [41]. The sol was stored at 5 °C and was aged for 2 days before being used in the experiment. All required solutions were prepared with distilled and deionized water from a Milli-Q-plus system of M/S Millipore Corp., USA.

2.2. Instrumentation

A Spex double monochromator (Model 1403) fitted with holographic gratings of 1800 grooves/mm and a cooled photomultiplier tube (Model R928/115) of Hamamatsu Photonics (Japan) were used for Raman spectra recording. The samples were taken in a quartz cell and were excited by 457.5-nm radiation from a Spectra Physics Ar^+ ion laser (Model 2020-05) at a power of 100 mW for the resonance Raman spectrum (RRS) in solution and as low as 50 mW for the SERS measurements to avoid sample degradation. Raman-scattered radiation was collected at a right angle to the excitation. The operation of the photon counter, data acquisition, and analysis were controlled by a Spex Datamate 1B. The acquisition time by the spectral element was 0.5 s. The scattered light was focused on the entrance slit of width of 4 cm^{-1}. All spectral measurements were made at least three times to ensure reproducibility. Polarized Raman spectra are recorded with an arrangement provided with the instrument. The accuracy in the measurement was ± 1 cm^{-1} for strong and sharp bands and slightly less for other bands. The electronic absorption spectra were recorded in a Shimadzu spectrophotometer Model UV–vis 2010 PC. The FTIR spectra of the powder samples were taken in a KBr pellet using a Nicolet Magna-IR 750 spectrometer series II. The resolution of the infrared bands was about 4 cm^{-1} for sharp bands and slightly less for broader bands. All the spectra reported in the figure are original raw data directly transferred from the instrument and processed using the Microcal origin version 4.10 16-bit program. They are presented even without single smoothing.

3. Results and discussion

3.1. NRS and FTIR spectra of H_2Tdpyp

The chemical structure of H_2Tdpyp is shown in Fig. 1a. Considering the 4-decylpyridyl as point masses, the H_2Tdpyp molecule has 38 atoms; hence, they have 108 fundamental vibrations. The molecule approximately belongs to the D_{2h} point group and under this symmetry the 108 fundamental

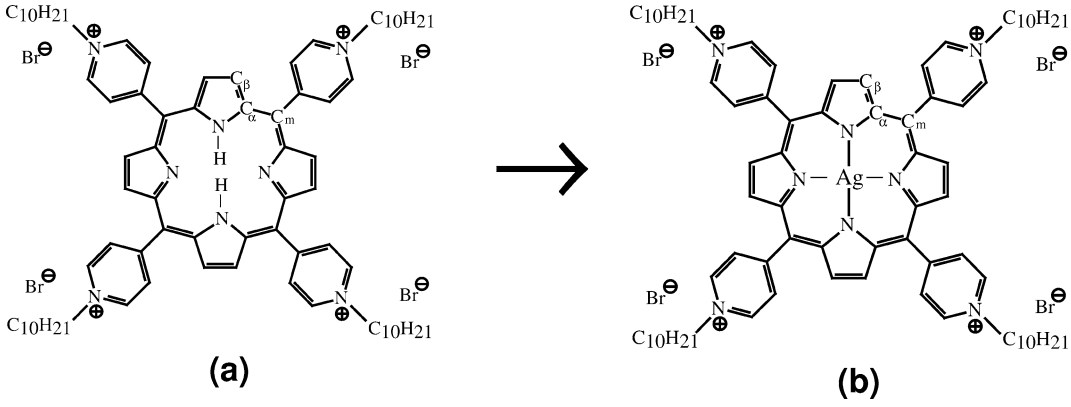

Fig. 1. Schematic representation of H_2Tdpyp or Por 10 molecule in (a) free state and (b) surface-adsorbed state.

vibrations of the molecule are classified as

$$\Gamma_{\text{vib}} = 19A_g + 18B_{1g} + 8B_{2g} + 9B_{3g} + 8A_u + 10B_{1u} + 18B_{2u} + 18B_{3u}.$$

Simple group theory predicts that all the g-modes are expected to be Raman active, while the u-modes are IR active. Among the g-modes 19 A_g modes are expected to be polarized in the Raman spectra.

Figure 2a shows the resonance Raman spectra (RRS) of powdered H_2Tdpyp in a KBr pellet and Fig. 2b that of 1.0×10^{-4} M aqueous solution obtained with Soret band (457.5 nm) laser excitation. Figure 2c shows the corresponding FTIR spectra of the powdered sample in a KBr pellet. Table 1 lists the FTIR, RR, and SERS band frequencies of the molecule along with their tentative assignments. In assigning the vibrational frequencies, literatures concerning with the RR and IR vibrational assignments of free-base and metalloporphyrins have been consulted extensively [7,16,18–20,41]. The modes arising mainly from the stretching, deformation, and bending vibrations of the core porphyrin skeleton and the externally substituted pyridyl group are easily identified. A 720-cm^{-1} band, assigned to a N–H out-of-plane bend of the two pyrrole rings in the porphyrin skeleton, appears as a moderately intense band in the FTIR spectra, but is absent in the Raman. Similarly, a medium intense band at 794 and 807 cm^{-1} assigned to a C_α–C_β–C_β stretch of pyrrole and pyrollenine ring, respectively, of the porphyrin macrocycle appear only in the FTIR spectra. Similar behavior is also observed for two degenerate modes at 1453 and 1461 cm^{-1}, which appear as strong signals only in the FTIR spectra. Interestingly, these intense modes are absent in the FTIR spectra of pure free-base porphin [42]. So its origin may well be from the externally attached pyridyl group. Considering the frequency region, we ascribed these modes to the in-plane C–C stretch of the externally attached pyridyl rings. The polarized 1257-cm^{-1} band (or 1254 cm^{-1} in solid) appears as a moderately intense band only in the RR spectra but is absent in the FTIR. This band is assigned to an in-plane C_m–pyridyl stretching vibration. Since the molecule is assumed to have a D_{2h} point group symmetry, it is expected that the Raman and IR vibrational modes will be complementary. However, analysis of the RR and the FTIR spectra show that the strong and polarized 1217-cm^{-1} mode in the RR spectra appears as a weak but prominent band in the FTIR. Similar behavior is observed for 1007-, 1297-, and 1560-cm^{-1} bands. Such anomalous behavior is also observed for 971-, 1170-, and 1640-cm^{-1} bands. All these modes appear as moderately strong or strong signals in both the RR and the FTIR spectra. The appearance of these modes in the RR and in the FTIR spectra may indicate different vibrational signatures in the same frequency region. This type of accidental degeneracy is not uncommon in such a complex molecule. Alternatively, if we consider the modes appearing both in the RR and in the FTIR spectra at the same frequency region, representing the same vibrational modes, then the porphyrin skeleton of the H_2Tdpyp molecule cannot be considered planar, and to have D_{2h} point group symmetry. The inversion center is to be considered lost, resulting in Raman activation of the infrared modes. The distortion in the porphyrin core macrocycle will make the molecule have a C_{2v} symmetry rather than D_{2h}. Considering the C_{2v} symmetry, the 108 fundamental vibrations of the molecule are now classified as

$$\Gamma_{\text{vib}} = 29A_1 + 26A_2 + 26B_1 + 27B_2.$$

With the molecule of C_{2v} symmetry, the Raman activation of all the IR modes is equally expected. However, we find that, except for certain modes, the complementary principle is obeyed. This may be an indication that the H_2Tdpyp molecule is more preferred to have a D_{2h} symmetry rather than C_{2v}. Moreover, 1007-, 1217-, 1297-, and 1560-cm^{-1} bands appear strong in the RR spectra, but weak in the FTIR. These features suggest that the porphyrin skeleton is nearly

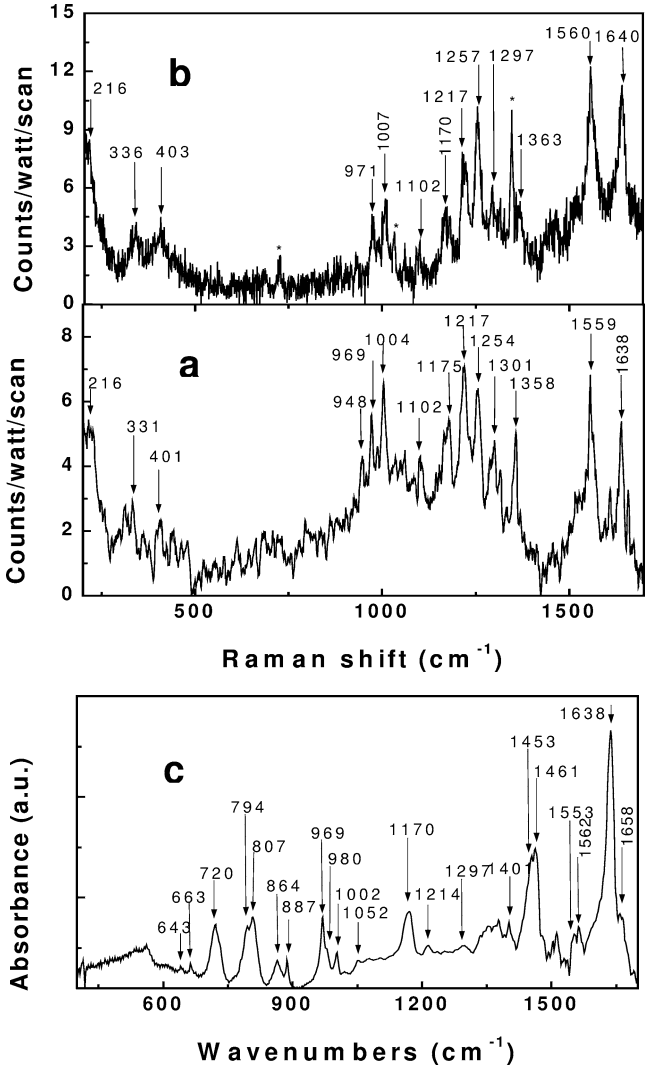

Fig. 2. (a) RRS of H_2Tdpyp of neat powder in KBr pellet and (b) in 1.0×10^{-4} M aqueous solution. All spectra are calibrated in counts/W/scan for $\lambda_{\text{exc}} = 457.5$ nm. (∗ Denotes the plasma lines.) (c) Background corrected FTIR spectra of H_2Tdpyp of neat powder in KBr pellet.

Table 1
Observed Raman and infrared bands of H_2Tdpyp in varied environments and their tentative assignments

FTIR in KBr pellet (cm^{-1})	RRS in KBr pellet (cm^{-1})	RRS in solution[a] (cm^{-1})	SERRS on Ag sol at 1×10^{-6} M cm^{-1}	Symmetry for D_{2h} (for C_{2v})	Tentative assignment[b]
	216 (vs)	216 (s)	224		Out-of-plane ring (X) tilting/Ag–N str.
	331 (w)	336 (w)	336		δ[ring (X)]
	401 (w)	403 (w)	401		γ[ring (X)]
643 (vw)					
663 (vw)					
720 (ms)				B_{1u} (A_1)	
807 (ms)				B_{3u} (B_1)	
864 (w)					
887 (w)					
	948 (ms)				
969 (ms)				B_{3u} (B_1)	
	969 (s)	971 (ms) P	968	A_g (A_1)	ν_s(C_α–C_m)
980 (sh)				B_{2u} (B_2)	
1002 (w)	1004 (vs)	1007 (ms) P	1006	A_g (A_1)	ν(Pyr)
1052 (vw/h)			1056		
	1102 (w)	1102 (w)	1098		δ_s(C_β–H)
1170 (ms)	1177 (s)	1170 (ms) P	1172	A_g (A_1)	ν(C_α–C_β) involving ring (X)
1214 (w)	1217 (vs)	1217 (s) P	1218	A_g (A_1)	δ(Pyr)
	1254 (vs)	1257 (ms) P	1255	A_g (A_1)	ν(C_m–Pyr)
1297 (w/h)	1301 (ms)	1297 (ms)	1296	A_g (A_1)	δ(Pyr)
1335 (vw/h)				B_{3u} (B_1)	
	1360 (s)	1363 (w)	1347	A_g (A_1)	ν_s(C_α–N) involving ring (X)
1401 (w)					
			1445		ν_s(C_α–C_β)
1453 (s)				B_{3u} (B_1)	ν(C–C)$_{pyr}$
1461 (s)				B_{2u} (B_2)	ν(C–C)$_{pyr}$
1553 (w)	1559 (vs)	1560 (vs) P	1553	A_g (A_1)	ν(C_β–C_β) involving ring (X)
1562 (w)					
1638 (vs)	1638 (vs)	1640 (vs) P	1639	A_g (A_1)	δ(Pyr)

[a] Abbreviations: P, polarized; vs, very strong; s, strong; ms, medium strong; w, weak; vw, very weak; sh, shoulder; h, hump.
[b] Abbreviations: ν, stretching; δ, in-plane bending/deformation; γ, out-of-plane folding; Pyr, external pyridyl group; subscript s denotes symmetric modes; ring (X) and ring (N) indicate the pyrrole and the pyrrolenine rings, respectively, of the porphyrin skeleton.

planar in the free state and has D_{2h} symmetry. Considering all the vibrational modes in the FTIR and RR and spectra, it could be concluded that the molecule is closer to having D_{2h} symmetry rather than C_{2v} symmetry.

In Table 1, it is shown that in the SERR spectra of the molecule in silver sol only the A_g modes of the D_{2h} symmetry or A_{1g} modes of the D_{4h} symmetry (as expected for the silver porphyrin molecule) are observed. This is in agreement with that reported by Hanzlikova et al. [4].

3.2. Concentration-dependent SERRS spectra

Figures 3a–3f show SERR spectra of the H_2Tdpyp molecule at varied concentrations in the range 1.0×10^{-5} to 5.0×10^{-7} M. It is observed that the overall SER signal increases as the concentration of the adsorbate molecule is lowered, attains a maximum at around 5.0×10^{-6}–1.0×10^{-6} M, and then decreases again with a further decrease in concentration. It is now well established that, on silver island films and in silver hydrosol, maximum enhancement is observed when a monolayer of the adsorbate molecule is formed on the surface and that as multilayers are formed the SER signal decreases [43,44]. It, therefore, seems plausible that the monolayer of the adsorbed H_2Tdpyp molecule is formed on the sol particles in the concentration range 5.0×10^{-6} to 1.0×10^{-6} M, which shows maximum enhancement of the SERR signal.

Considering the entire concentration-dependent profile (Figs. 3a–3f), we find that the concentration range between 1.0×10^{-5} and 5.0×10^{-7} M is most sensitive not only for large signal counts but also for interesting variations in the relative intensities of certain observed bands. Such intensity variations are observed in the 1255-, 1347-, 1552-, and 1640-cm^{-1} bands. The first three bands are assigned to ν(C_m–Pyr), ν(C_α–N), ν(C_β–C_β), respectively, of the porphyrin skeleton and the 1640-cm^{-1} band is assigned to the in-plane bending or deformation of the external pyridyl ring. Intensity reversal occurs between 1255- and 1347-cm^{-1} bands and also between 1553- and 1640-cm^{-1} bands as the adsorbate concentrations change from 5.0×10^{-6} to 5.0×10^{-7} M. As the concentration changes from 5.0×10^{-6} to 5.0×10^{-7} M, the 1640-cm^{-1} band enhances by a factor of 8.0, whereas the 1553-cm^{-1} band enhances by a factor of 4.0 only, which results in intensity reversal between the two bands. On lowering of the concentration

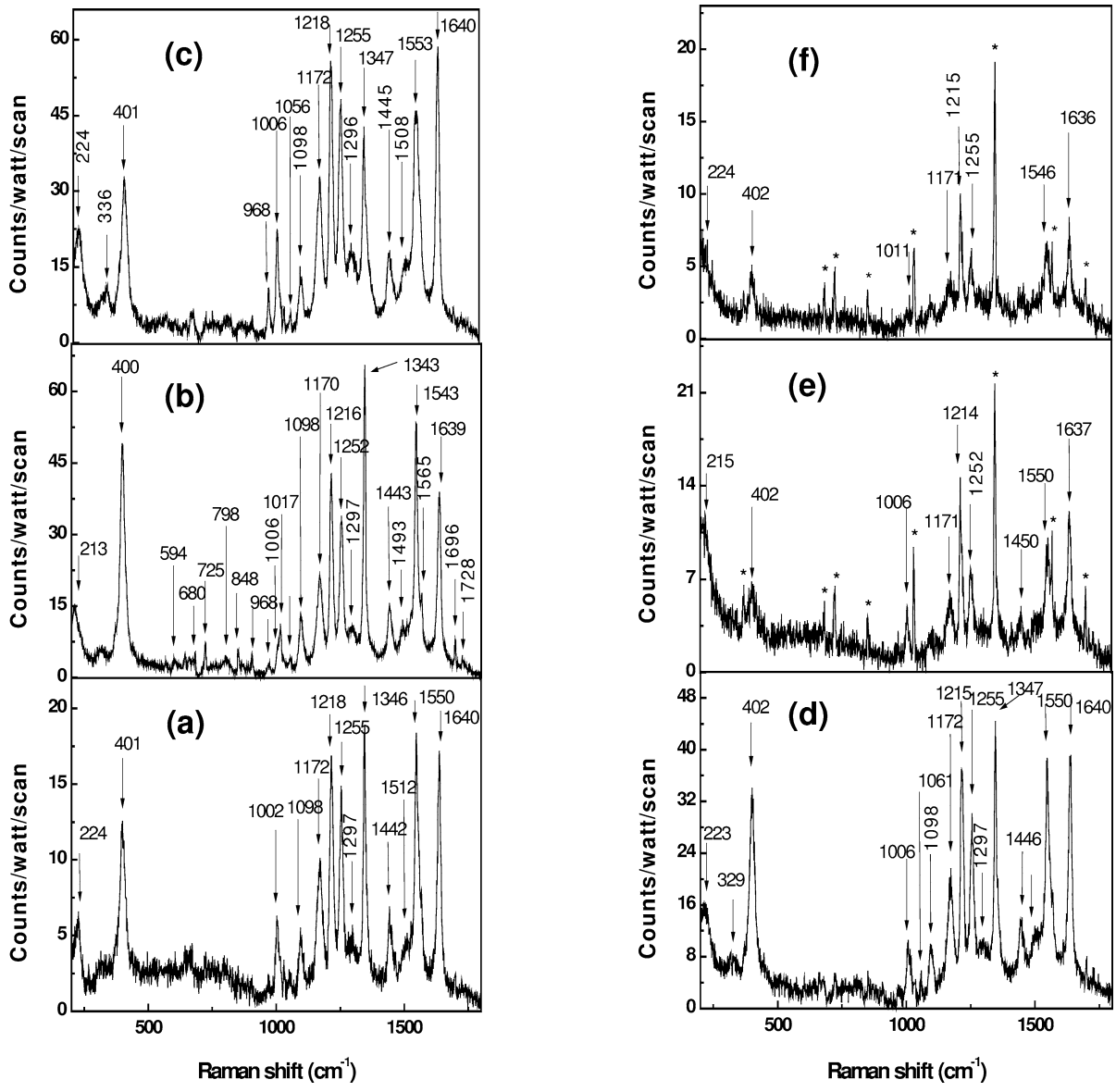

Fig. 3. SER spectrum of H_2Tdpyp adsorbed in silver hydrosol at concentrations (a) 1.0×10^{-5} M, (b) 5.0×10^{-6} M, (c) 1.0×10^{-6} M, (d) 5.0×10^{-7} M, (e) 1.0×10^{-7} M, and (f) 1.0×10^{-8} M for $\lambda_{exc} = 457.5$ nm. (∗ Denotes the plasma lines.)

further to 5.0×10^{-7} M, the enhancement of the 1640-cm^{-1} band occurs by a factor of 1.3, whereas the enhancement of the 1553-cm^{-1} band is by a factor of 1.7, thus again showing intensity reversal and thus making both the bands nearly equally intense. Similar behavior is also observed for the band pairs at 1255 and 1347 cm^{-1}. Such intensity variation of SERR spectra with adsorbate concentration has been attributed to the change in the orientation of the molecule on the silver surface [33–39].

The other striking feature of the SERR spectra is the huge enhancement of the 401-cm^{-1} band, assigned to the out-of-plane folding of the pyrrole rings of the porphyrin skeleton [7,26] as the concentration is increased to 5.0×10^{-6} M. Intense 401-, 1343-, and 1552-cm^{-1} modes in the SERR spectra are considered as sensitive markers of metalloporphyrins and, more specifically, are the indication of Ag(II)Tdpyp complex formation [4–25,27–30]. Silver incorporation in to the H_2Tdpyp molecule adsorbed on silver colloids is rather facile and it follows as [25,45]

$$H_2\text{Tdpyp} + \text{Ag} \Rightarrow \text{Ag(II)Tdpyp} + 2\text{H}^+.$$

It is known that complete metallation of H_2Tdpyp is achieved very rapidly on adsorption of this type of molecule on a borohyride-reduced silver colloid [4]. This is verified from the time-dependent study, where the SER spectral features remain identical, even when it is recorded a few hours after the preparation of the sample. Thus, Ag(II)Tdpyp eventually represents a metalloporphyrin, shown in Fig. 1b, which in the free state has a D_{4h} point group symmetry. Thus, the SERR spectra of H_2Tdpyp are the spectra of silver–porphyrin obtained from its free-base counterpart.

In the entire concentration-dependent profile, we observe a moderately intense band near the 224-cm^{-1} regions. In SER spectral analysis, this frequency range is often identified as a Ag–N stretching vibration [46–48]. Incidentally, around this frequency range at 216 cm^{-1} an intense and a moderately intense band are observed in the NRS of the bulk and in solution, respectively. This band is assigned to pyrrole tilting mode [26]. However, considering the bandwidth of the 224-cm^{-1} mode we believe that both Ag–N and pyrrole tilting modes may remain overlapped and could not be identified separately.

Though it is quite difficult to enumerate the orientation of such a complicated molecule, to have a precise idea regarding the orientation of a molecule with concentration, we estimate the apparent enhancement factors (AEF) of some selected Raman bands using the relation we used before [49]. Accordingly,

$$\mathrm{AEF} = \sigma_1 C_2/\sigma_2 C_1, \tag{1}$$

where subscripts 1 and 2 refer to SER and NR spectra, respectively, and C and σ represent the concentration of the molecule and peak heights of the Raman bands calibrated in counts/W/scan measured from the baseline. They are shown in Table 2. The real enhancement factor is a few orders of magnitude higher than that shown in Table 2 [46]. Orientation of the adsorbed molecule on the metal surface is estimated from the enhancement of the relevant Raman bands following the surface selection rule based on image dipole theory as predicted by Creighton et al. [41] and Allen and Van Duyne [50].

It is clearly seen from Table 2 that we obtain a moderate 1 order enhancement of all the bands representing in-plane vibrations at a concentration of 1.0×10^{-5} M that increases by 1 order at 5.0×10^{-7} M. This may indicate that the porphyrin skeleton with its external pyridyl group is nearly parallel to the silver surface. The nearly flat orientation of the porphyrin core is substantiated by the weak enhancement of the 1550-cm^{-1} mode, assigned to in-plane C_β–C_β stretching of the pyrrole rings of the porphyrin skeleton. Weak enhancement of 1172-, 1218-, and 1640-cm^{-1} bands are all assigned to in-plane bending or deformation of the external pyridyl group supports in favor of its nearly flat orientation on the colloidal silver surface along with the porphin skeleton.

Table 2
Apparent enhancement factors of some selected Raman bands of H_2Tdpyp at various concentrations

RRS of soln. (cm^{-1})	1×10^{-5} M	5×10^{-6} M	1×10^{-6} M	5×10^{-7} M
403	4.21×10^1	3.72×10^2	1.18×10^2	2.38×10^3
971	–	1.23×10^1	2.33×10^2	3.82×10^2
1007	1.16×10^1	–	4.26×10^2	3.96×10^2
1170	2.12×10^1	8.81×10^1	6.54×10^2	8.77×10^2
1217	2.15×10^1	1.64×10^2	7.25×10^2	9.41×10^2
1257	1.45×10^1	1.40×10^1	4.71×10^2	5.95×10^2
1560	1.58×10^1	8.8×10^1	3.84×10^2	6.31×10^2
1640	1.42×10^1	6.8×10^1	5.29×10^2	6.94×10^2

At 5.0×10^{-6} M, we obtain 2-order enhancement of the 400-cm^{-1} band. Compared to the in-plane modes, the 401-cm^{-1} band assigned to out-of-plane folding of the pyrrole ring of the porphyrin core, is enhanced more. The enhancement of 1343- and 1550-cm^{-1} bands, assigned to in-plane C_α–N and C_β–C_β stretching, respectively, also indicate that the pyrrole rings of the porphyrin skeleton are not exactly planar. This loss of planarity may be due to the force of attraction of the central silver atom. At this concentration we obtain a similar type of enhancement for 1170- and 1216-cm^{-1} bands ascribed to in-plane bending or deformation of the external pyridyl groups. This indicates that the pyridyl groups are not exactly flat but remain somewhat tilted on the silver surface.

At 1.0×10^{-6} M concentration of the adsorbate, the enhancement of all the modes increases slightly but the general behavior of various modes remains the same. At 5.0×10^{-7} M, we estimated 3 orders of magnitude enhancement for the 402-cm^{-1} band, which indicate that the orientation of the porphyrin core remain nearly flat. Enhancement of 1343- and 1550-cm^{-1} bands again indicates that the pyrrole rings of the porphyrin skeleton are not exactly planar but are tilted. Moderate 2-orders enhancement of 1006-, 1255-, and 1640-cm^{-1} bands, assigned to pyridyl ring breathing, in-plane bending, or deformation of C_m–Pyr and pyridyl ring, respectively, along with similar enhancement of 1218-cm^{-1} modes, indicate significant tilt of the external pyridyl groups.

Thus, from the entire concentration-dependent profile, we believe that the core porphyrin skeleton remains almost flat on the silver surface with the pyrrole rings somewhat tilted, but the external pyridyl ring changes its tilt angle with the adsorbate concentration. This is manifested in the alteration of relative band intensity of 1640- and 1550-cm^{-1} bands and 1347- and 1255-cm^{-1} bands.

Considering the flat orientation of the H_2Tdpyp molecule, we estimated the amount of porphyrin molecules required for monolayer coverage on silver colloidal particles present in 1c.c. of the colloidal system. It has been enumerated using the relation reported by Prochazka et al. [4]. Accordingly,

$$n = \frac{3FW_{\mathrm{Ag}}}{N_A r S \delta_{\mathrm{Ag}}} V C_{\mathrm{Ag}}. \tag{2}$$

where n is the number of porphyrin molecules required for monolayer coverage, FW_{Ag} and δ_{Ag} are the formula weight and density of silver, respectively, C_{Ag} is the molar concentration of Ag in colloidal solution, N_A is Avogadro's number, r is the average radius of the colloidal particles, S is the surface covered by a single adsorbate molecule, and V is the volume of the sample. The C_{Ag} for our present colloidal system is 2.36×10^{-4}, and the average radius (r) of the colloidal particles is around 25 nm. If we consider the diameter of the H_2Tdpyp molecule approximately to be around 2.6 nm, then the amount of porphyrin molecules required for monolayer coverage is about 20,000 pmol. That corre-

sponds to 2.0×10^{-7} M concentration. This is in agreement with our experimental results, which shows near-flat orientation of the porphyrin core at 5.0×10^{-7} M concentration.

3.3. Electronic absorption of silver colloid with added H_2Tdpyp

Figures 4a and 4b show the electronic absorption spectra of 1.0×10^{-4} M H_2Tdpyp in aqueous solution and the Ag sol before and after the addition of H_2Tdpyp at different concentrations, respectively. The pure stable silver sol shows a single extinction maximum at 392 nm. When 5×10^{-6} M of H_2Tdpyp is added to the sol, the absorption spectra resemble those of pure sol; the only difference is that the extinction maximum at 392 nm is reduced somewhat. Upon the addition of 1.0×10^{-6} M of H_2Tdpyp, the absorbance of the initial sol band is reduced further with the appearance of a new distinct shoulder at around 448 nm. However, at 5.0×10^{-7} M concentration, a significant decrease in intensity of the initial sol band is observed and the absorbance in the higher wavelength region gains further intensity and appears as a broad band centered at around 629 nm. Thus, we see a gradual red shift of the higher wavelength band with a decrease in molecular concentration of the adsorbate. The appearance of such a broad band in the higher wavelength region is attributed to the aggregation of spherical colloidal silver particles of the sol in the presence of the adsorbed molecules [41,51] and its gradual red shift signifies the state of aggregation at various adsorbate concentrations [52]. Alternatively, such a band in the NIR region of the extinction spectra has been ascribed to a charge transfer (CT) band due to the molecule–metal interaction [53–56]. Though the higher wavelength bands at 448 and 629 nm did not undergo any shift for several hours, the gradual red shift of this band with the adsorbate concentration forces us to think its origin is due to the coagulation of the silver particles rather than CT contribution. However, the disappearance of the broad band in the higher wavelength region may also be due to the sedimentation of the colloidal aggregates from the system [24].

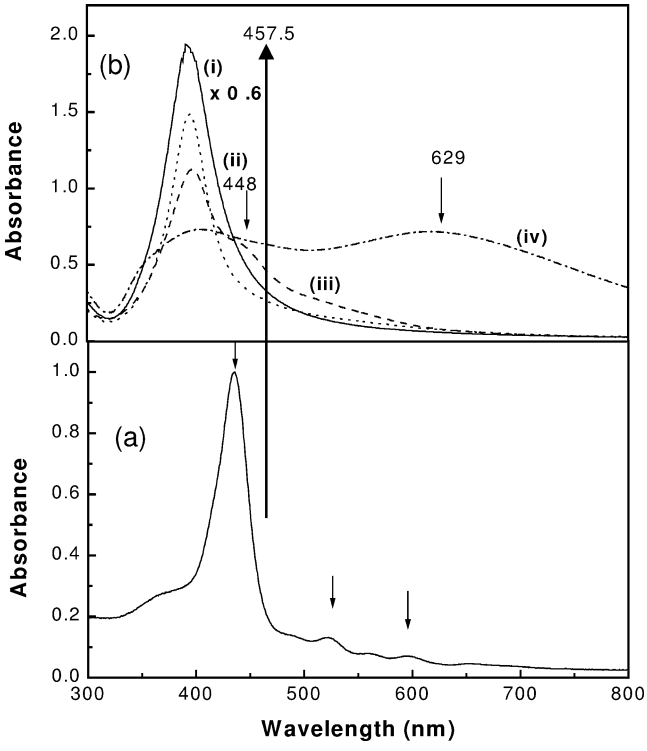

Fig. 4. Room-temperature normalized UV–vis absorption spectra of (a) a 1.0×10^{-4} M aqueous solution of H_2Tdpyp and (b) UV–vis absorption spectra of (i) pure silver sol without and with H_2Tdpyp at (ii) 5.0×10^{-6}, (iii) 1.0×10^{-6}, and (iv) 5.0×10^{-7} M concentrations.

3.4. Excitation wavelength dependence

We investigated the excitation wavelength dependence of the SER spectra of H_2Tdpyp at 5×10^{-6} M molecular concentration. In Figs. 5a–5e, we show the SER spectra at different excitation frequencies available from our Ar^+ laser. It is observed that almost all the bands increase in intensity as the excitation wavelength is decreased from 514.5 to 457.5 nm. This variation for the three well-resolved

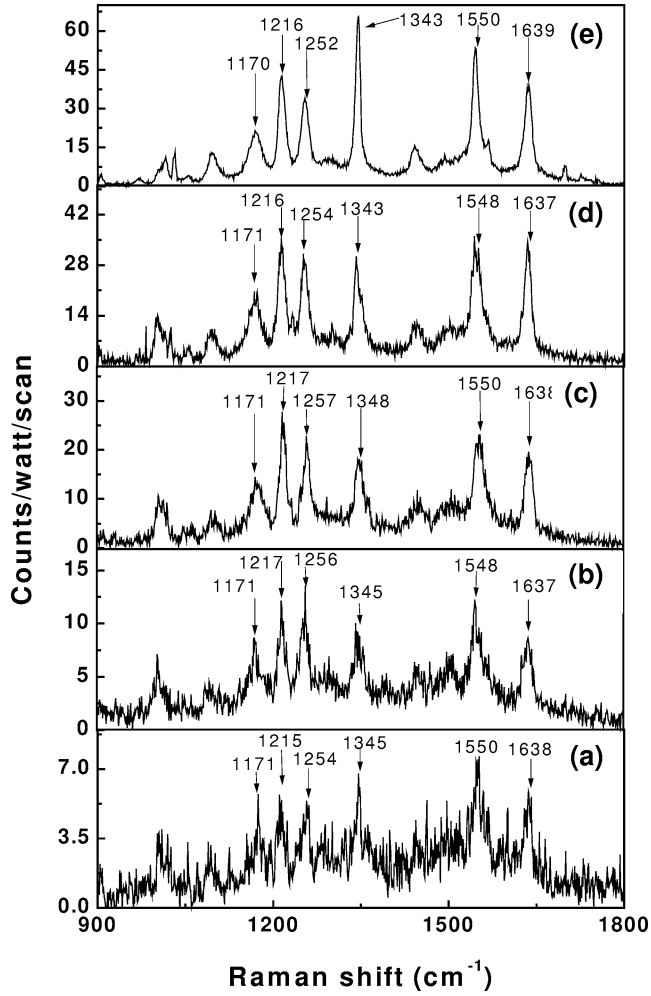

Fig. 5. Excitation wavelength dependence of the SER spectra at 5.0×10^{-6} M of H_2Tdpyp for wavelengths (a) 514.5, (b) 496.5, (c) 488, (d) 476.5, and (e) 457.5 nm.

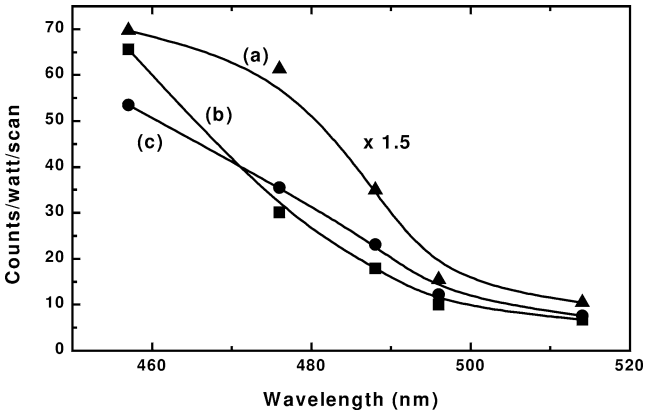

Fig. 6. Excitation wavelength dependence of (a) 1343-, (b) 1550-, and (c) 1639-cm^{-1} band intensity calibrated in counts/W/scan for an H_2Tdpyp molecule.

prominent bands at 1343, 1550, and 1639 cm^{-1} are shown in Fig. 6. Thus, we have seen that the surface enhancement for all the bands of the H_2Tdpyp molecule increases as the excitation radiation shifts toward the plasmon resonance wavelength of the Ag sol. With our experimental limitation, we observed maximum enhancement on excitation with 457.5-nm radiation of an argon ion laser, the shortest wavelength available to us. This indicates that the classical electromagnetic effect contributes more in the SER spectra of the H_2Tdpyp molecule.

4. Conclusion

The RR and the FTIR spectra of the H_2Tdpyp molecule have been compared and the analysis indicates that the molecule in its free state has nearly D_{2h} symmetry rather than C_{2v}. In the surface-adsorbed state in silver sol, the SERR spectra suggest metallation of the molecule, which results in a more symmetric (D_{2h}/D_{4h}) silver porphyrin molecule.

The concentration-dependent SER spectra have been studied. The variation in the relative intensities of the Raman bands with the adsorbate concentration is attributed to the change in molecular orientation. However, in general, the overall SER spectra are characterized by the intensification of certain specific bands, which are considered to be the metallation markers of metallated porphyrins. This adds further credence to the formation of metallo (silver) porphyrin on adsorption on colloidal silver particles.

The broad band in the long wavelength region of the electronic absorption spectra of the sol with added adsorbate at various concentrations has been explained in terms of the aggregation of the colloidal silver particles. From the excitation wavelength dependence study, it is observed that as the excitation wavelength is moved toward the plasmon resonance wavelength of the Ag sol, the enhancement increases. This indicates that the classical electromagnetic effect contributes more toward the SERS of the H_2Tdpyp molecule.

Acknowledgments

The authors express there thanks to DST, Government of India, for financial support. Special thanks are due to Professor G.B. Talapatra of our Department and Professor P.K. Mallick of the Physics Department, Burdwan University, for their continuous encouragements and stimulating and constructive discussions.

References

[1] M.Y. Okamara, G. Feher, N. Nelson, in: Govindjee (Ed.), Photosynthesis, Academic Press, New York, 1982, p. 195.
[2] G. Feher, M.Y. Okamara, in: R.K. Clayton, W.R. Sistrom (Eds.), The Photosynthetic Bacteria, Plenum, New York, 1978, p. 349.
[3] H.T. Witt, in: H. Gerisher, J.J. Katz (Eds.), Light-Induced Charge Separation in Biology and Chemistry, VCH, Weinheim, 1979, p. 303.
[4] J. Hanzlikova, M. Prochazka, J. Stepanek, J. Bok, V. Baumruk, P. Anzenbacher Jr., J. Raman Spectrosc. 29 (1998) 575.
[5] M. Prochazka, J. Stepanek, P.Y. Turpin, J. Bok, J. Phys. Chem. B 106 (2002) 1543.
[6] C.L. Honeybourne, J. Phys. Chem. Solids 48 (1987) 109.
[7] P. Stein, A. Ulman, T.G. Spiro, J. Phys. Chem. 88 (1984) 369.
[8] R.A. Reed, R. Purrello, K. Prendergast, T.G. Spiro, J. Phys. Chem. 95 (1991) 9720.
[9] V.A. Walters, J.C. Paul, G.T. Babcock, G.E. Leroi, J. Am. Chem. Soc. 111 (1989) 8300.
[10] E.W. Findsen, J.A. Shelnutt, M.R. Ondrias, J. Phys. Chem. 92 (1988) 307.
[11] A.L. Verma, H.J. Bernstein, J. Chem. Phys. 61 (1974) 2560.
[12] E.W. Findsen, J.A. Shelnutt, J.M. Friedman, M.R. Ondrias, Chem. Phys. Lett. 126 (1986) 465.
[13] A.L. Verma, H.J. Bernstein, Biochem. Biophys. Res. Commun. 57 (1974) 255.
[14] S. Sunder, H.J. Bernstein, J. Raman Spectrosc. 5 (1976) 351.
[15] K.N. Solovyov, L.L. Gladkov, A.T. Gradyushko, N.M. Ksenofontova, A.M. Shulga, A.S. Starukhin, J. Mol. Struct. 45 (1978) 267.
[16] X. Li, R.S. Czernuszewicz, J.R. Kincaid, Y. Su, T.G. Spiro, J. Phys. Chem. 94 (1990) 31.
[17] L.L. Gladkov, K.N. Solovyov, Spectrochim. Acta A 41 (1985) 1443.
[18] N. Blom, J. Odo, K. Nakamoto, D.P. Strommen, J. Phys. Chem. 90 (1986) 2847.
[19] D.L. Willems, D.F. Bacian, J. Phys. Chem. 89 (1985) 234.
[20] J.M. Birke, J.R. Kincaid, T.G. Spiro, J. Am. Chem. Soc. 100 (1978) 6077.
[21] R.P. Van Duyne, in: C.B. Moore (Ed.), Chemical and Biological Applications of Lasers, Vol. 4, Academic Press, New York, 1979, p. 101.
[22] A. Otto, in: M. Cardona, G. Gunthecodt (Eds.), Light Scattering in Solids, Vol. 4, Springer-Verlag, New York, 1984, p. 289.
[23] C.A. Murray, in: R.K. Chang, T.E. Furtak (Eds.), Surface-Enhanced Raman Scattering, Plenum, New York, 1982, p. 203.
[24] P. Mojzes, B. Vickova, P.-Y. Turpin, J. Phys. Chem. B 101 (1997) 3161.
[25] A.H.R. Al-Obaidi, S.J. Rigby, S.E.J. Bell, J. McGarvey, J. Phys. Chem. 96 (1992) 10960.
[26] O.K. Song, M.J. Yoon, D. Kim, J. Raman Spectrosc. 20 (1989) 739.
[27] K. Itoh, T. Sugii, M. Kim, J. Phys. Chem. 92 (1988) 1568.
[28] M. Kim, T. Tsujino, K. Itoh, Chem. Phys. Lett. 125 (1986) 364.
[29] Y. Kobayashi, K. Itoh, J. Phys. Chem. 89 (1985) 5174.
[30] K. Shoji, Y. Kabyashi, K. Itoh, Chem. Phys. Lett. 102 (1983) 179.
[31] P. Mojzes, J. Pfleger, J. Mol. Struct. 482–483 (1999) 225.
[32] X.-Y. Li, V.I. Petrov, D. Chen, N.-T. Yu, J. Raman Spectrosc. 32 (2001) 503.

[33] S.K. Kim, T.H. Joo, S.W. Suh, M.S. Kim, J. Raman Spectrosc. 17 (1986) 381.
[34] M. Moskovits, J.S. Suh, J. Phys. Chem. 92 (1988) 6327.
[35] T.H. Joo, K. Kim, M.S. Kim, J. Phys. Chem. 90 (1986) 5816.
[36] M. Takahashi, M. Ito, Chem. Phys. Lett. 103 (1984) 512.
[37] M. Takahashi, Y. Sakai, M. Fujita, M. Ito, Surf. Sci. 176 (1986) 351.
[38] M. Takahashi, M. Fujita, M. Ito, Chem. Phys. Lett. 109 (1984) 122.
[39] J. Chowdhury, M. Ghosh, T.N. Misra, to be published.
[40] Y. Okino, W.E. Ford, M. Kelvin, Synthesis 1 (1980) 537.
[41] J.A. Creighton, C.G. Blatchford, M.G. Albrecht, J. Chem. Soc. Faraday Trans. 2 75 (1979) 790.
[42] L.L. Gladkov, A.T. Gradyushko, A.M. Shulga, K.N. Solovyov, A.S. Starukhin, J. Mol. Struct. 47 (1978) 463.
[43] P.N. Sanda, J.M. Warlaumont, J.E. Demuth, J.C. Tsang, K. Christmann, J.A. Bradley, Phys. Rev. Lett. 45 (1980) 1519.
[44] U.K. Sarkar, A.J. Pal, S. Chakraborti, T.N. Misra, Chem. Phys. Lett. 190 (1992) 59.
[45] A.D. Alder, F.R. Longo, F. Kampas, J. Kim, J. Inorg. Nucl. Chem. 32 (1970) 2443.
[46] K.M. Mukherjee, T.N. Misra, J. Raman Spectrosc. 27 (1996) 595.
[47] U.K. Sarkar, S. Chakrabarti, T.N. Misra, J. Raman Spectrosc. 24 (1993) 97.
[48] H. Wetzel, H. Gerischer, B. Pettinger, Chem. Phys. Lett. 78 (1981) 392.
[49] K.M. Mukherjee, D. Bhattacharjee, T.N. Misra, J. Colloid Interface Sci. 193 (1997) 286.
[50] C.S. Allen, R.P. Van Duyne, Chem. Phys. Lett. 63 (1979) 455.
[51] C.G. Blatchford, J.R. Campbell, J.A. Creighton, Surf. Sci. 120 (1982) 435.
[52] S. Sanchez-Cortes, J.V. Gracia-Ramos, G. Morcillo, J. Colloid Interface Sci. 167 (1994) 428.
[53] H. Yamada, in: H.D. Bist, J.R. Durig, J.F. Sullivan (Eds.), Raman Spectroscopy: Sixty Years on Vibrational Spectra and Structure, Vol. 17A, Elsevier, Amsterdam, 1989, p. 391.
[54] S. Sanchez-Cortes, J.V. Gracia-Ramos, G. Morcillo, A. Tinti, J. Colloid Interface Sci. 175 (1995) 358.
[55] J. Chowdhury, M. Ghosh, T.N. Misra, J. Colloid Interface Sci. 228 (2000) 372.
[56] J. Chowdhury, M. Ghosh, T.N. Misra, Spectrochim. Acta A 56 (2000) 2107.